Materials Research Proceedings 41 (2024) 2648-2657 https://doi.org/10.21741/9781644903131-290

Two-step forging of polyimide powders into small-/medium-sized gears with and without carbon fiber reinforcement

AIZAWA Tatsuhiko[1,a*], MIYATA Tomohiro[2,b] and ENDO Kiyoyuki[3,c]

[1]3-15-10 Minami-Rokugo, Ota-City, Tokyo 144-0045, Japan

[2]215-1 Monden Industrial Park, Aizu-Wakamatu, Fukushima 965-0846, Japan

[3]4-1-5 Sannoh, Ota-City, Tokyo 143-0023, Japan

[a]taizawa@sic.shibaura-it.ac.jp, [b]aizu5@marutaka-ind.co.jp, [c]endo@igma.co.jp

Keywords: Polyimide Powder Feed Stock, Green Preform, Sinter-Forging, Carbon Reinforcement

Abstract. A green polyimide cylindrical preform with short carbon fibers was prepared for two-step forging processes. Each preform was hot-forged at 623 K above the glass transition temperature of polyimide for near-net shaping of fifteen-teeth module-1.0 gear, and sinter-forged at 673 K below its melting point for densification. SEM and X-ray computer tomography were employed to make destructive and non-destructive diagnoses on the carbon fiber orientation during hot forging. Micro-hardness testing and gear-grade balancing were utilized to evaluate the engineering durability and dimensional accuracy of sinter-forged gears.

Introduction

Light weight and high stiffness have become an essential key item for mechanical gears in the reducers of the robotics and electrical vehicles [1]. Minimization of gear volume without change of loading capacity and mechanical constraints is the first approach to reduce the weight of mechanical parts and elements [2]. In case of the gear design, the weight can be reduced only with the decrease of stiffness [3]. The light weight metals, alloys and plastics are employed as the second approach to decrease the weight without loss of stiffness [4]. The carbon fiber reinforced gears and screws could provide the solution [5]; the long carbon fibers are difficult to be aligned after plastic flow into the gear matrix [6]. In addition, the polymer matrix property has often less engineering durability in severe conditions with heating up on the contact interface. New approach is necessary to satisfy the light weight, the high stiffness and the engineering toughness as a gear to be working even in severe situation [7-8].

Authors proposed the super-engineering plastic gears with the higher melting point than 700 K, the higher strength and toughness than the conventional CFRP (Carbon Fiber reinforced plastics) and CFRTP (Carbon Fiber Reinforced Thermo-Plastics) [9-10]. Two step PM (Powder Metallurgy) procedure was also developed to make a gear-shaped green compact and to sinter-forge this green compact to a net-shaped gear. This sinter-forged gear had a well-defined gear-grade balance; e.g., the cumulative pitch deviation was fixed into -10 μm to +10 μm. This deviation for fifteen teeth gear without finishing was classified into JIS-2 grade.

In the present study, the carbon fibers are included and mixed into the polyimide powders to build up the feedstock. This mixture powders are poured into a die cavity for cold compaction to a cylindrical green preform. This preform is hot forged above the glass transition temperature to a fifteen teeth gear model. During this viscous matrix flow, the carbon fibers are forced to orient along the plastically flowing directions of matrix. The hot forged model is further sinter-forged to a net-shaped fifteen teeth gear. SEM (Scanning Electron Microscopy) and XCT (X-ray Computer Tomography) are utilized to make destructive and non-destructive diagnoses on the orientation of carbon fibers in the polyimide matrix during the hot forging of green compact. Micro-Vickers hardness testing was employed to measure the hardness of tooth top and bottom of sinter-forged

fifteen teeth gear. In the above three processes, CNC (Computer Numerical Control) stamper was commonly utilized with and without use of IH (Induction Heating) units to keep the specified holding temperature. The gear-grade evaluation is also performed to measure the dimensional deviations of tooth shape and geometry.

Methods and Materials

The green compaction, the hot forging and the sinter forging processes are explained in detail to point out the processing parameters in each process.

Green compaction to preforms. The recycled long carbon fibers from the CFRP in-factory dusts, were used as a feed stock. These fibers were cut into chips with the length of 5 mm in average. Their weight was measured to determine their total mass for inclusion into the green compact.

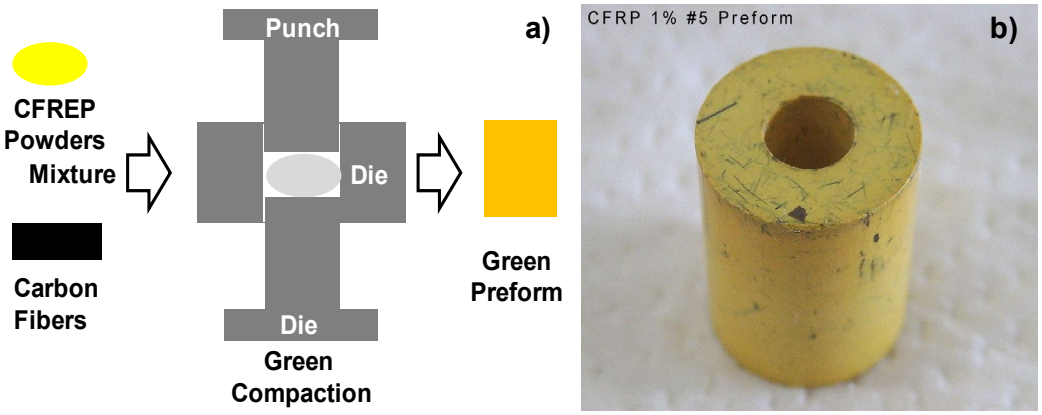

Figure 1. Green compaction process to consolidate the powder mixtures with carbon short fibers into a preform. a) Schematic view on the die-set for consolidation process, and b) a cylindrical preform of consolidated polyimide powders with short carbon fibers.

The measured carbon fiber - polyimide powder mixture, was poured into a die cavity in the cold compaction die - punch unit in Fig. 1a. The load was applied by 3 kN to yield the green compact with the relative density of 70 to 80% for the true polyimide density.

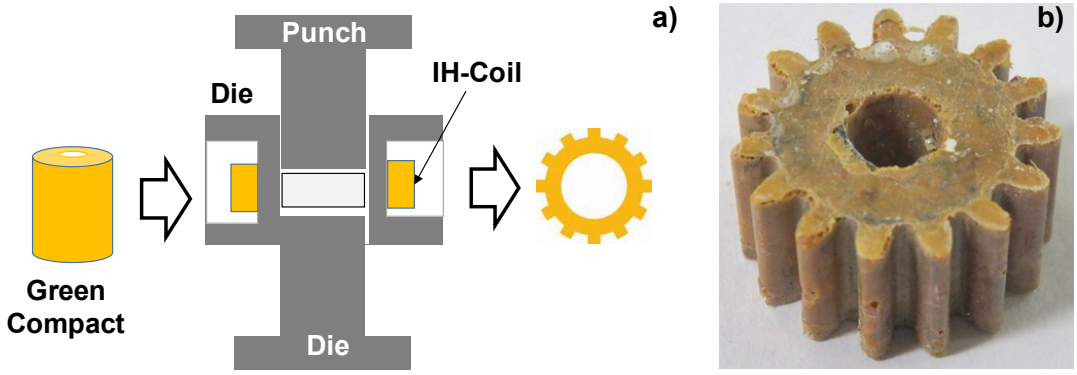

Figure 2. Hot forging of the preform to gear-shaped intermediates. a) Schematic view on the die-set for hot forging, and b) a gear-shaped product intermediate.

Two-step PM-forging processes. PM-forging process consists of two steps. At first, the hot PM-forging is utilized to make near-net shaping of the preform to a gear model with fifteen teeth, module 1.0 above the glass-transition temperature of polyimide matrix. Through this viscous deformation and flow of polyimide matrix, the short carbon fibers are realigned from the original locations to the tooth tops together with this matrix flow. Fig. 2a illustrates the experimental setup

for this hot forging. IH-coil was used for heating and holding temperature after thermal transient program. The uniaxial compression load was applied during hot forging step. The holding time as well as the applied load were varied to investigate their effect on the plastic flow of polyimide matrix. Fig. 2b depicts the hot forged fifteen teeth, module 1.0 gear model.

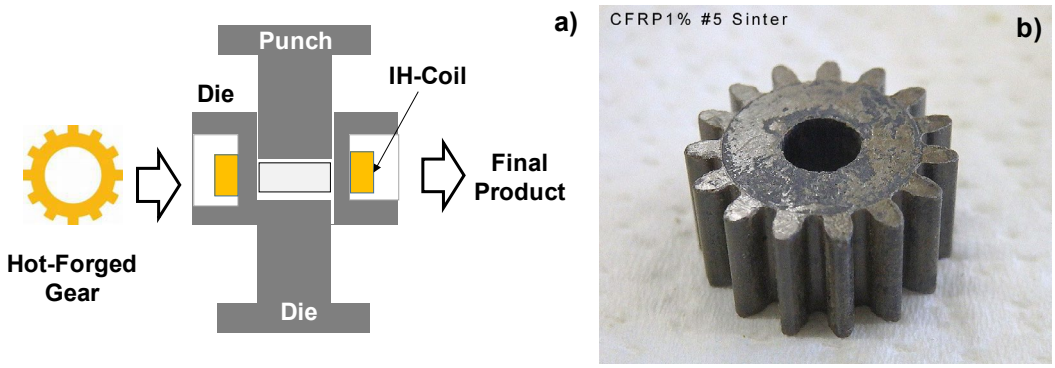

Figure 3. Sinter forging of the gear-shaped intermediates to the final product before polishing. a) Schematic view on the die-set for sinter forging, and b) a gear-shaped product before polishing.

The sinter-forging was utilized as the second step for densification below the melting point of polyimide matrix. Fig. 3a illustrates the similar setup to the hot forging. In practical operation, both forging steps were performed in the successive manner without ejection of forged sample. After the time schedule in the CNC stamping unit, the loading and temperature sequences were controlled in practice before cooling. Fig. 3b shows the final product with the outer diameter of 16.4 mm, the inner diameter of 11.9 mm and PCD of 14.2 mm after sinter-forging,

Work materials. The polyimide powders (Aurum; Mitsui Chemicals, Co., Ltd.) were shown in Fig. 4a. This Aurum-PD450 was a thermoplastic polyimide with T_g (Glass transition temperature) of 518 K (or 245 °C), T_m (Melting temperature) of 661 K (or 388 °C), and the density of 1.33 g/cm^3. The carbon long fibers with the density of 2.0 g/cm^3, were recycled from the CFRP (Carbon fiber reinforced plastic) in-factory dusts, as shown in Fig. 4b. These fibers were cut into short fibers with the length of 5 mm.

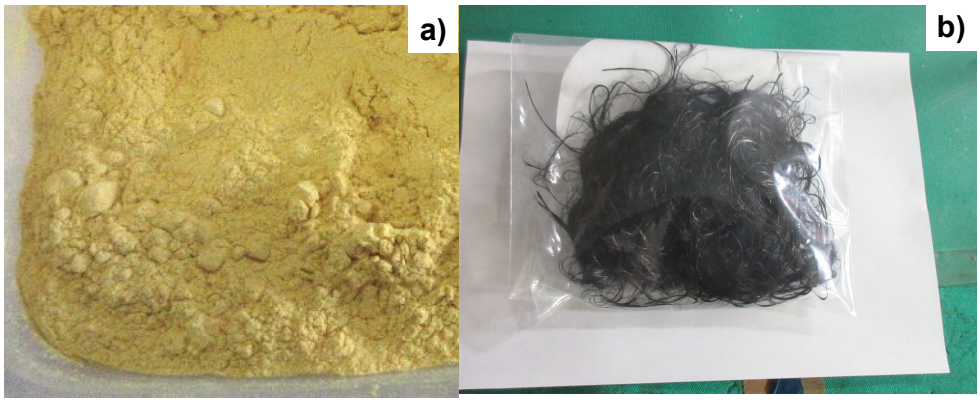

Figure 4. Initial feedstock of work materials. a) Polyimide powders, and b) recycled carbon fibers from CFRP dusts.

These short fibers were mixed with the polyimide powders to prepare the starting material for green compaction and successive forging processes. The mass fraction of carbon fibers was varied to be 1, 3 and 5 mass% against the polyimide powder mass.

Materials Research Proceedings 41 (2024) 2648-2657 https://doi.org/10.21741/9781644903131-290

Characterization. The micro-Vickers hardness testing was employed to optimize the forging process parameters such as the alloyed load and loading duration. SEM (Scanning Electron Microscopy; JOEL, Tokyo, Japan) and XCT (X-ray Computer Tomography) were utilized for destructive and non-destructive diagnosis on the green compact and the sintered gears to describe the alignment of carbon fibers.

Results

The green compaction is performed to prepare the preform for hot- and sinter-forging processes. This two-step forging is utilized to yield the carbon fiber reinforced polyimide gears with varying the carbon fiber contents.

Polyimide – carbon fiber preform by green compaction. The mixture polyimide powders with the short carbon fibers were consolidated to a green preform by cold compaction, as depicted in Fig. 1. The applied load was 3 kN and the constant velocity was 0.1 m/s. The cylindrical preform had the relative density of 70-80%. In addition to the destructive evaluation by SEM, the XCT was utilized to make nondestructive diagnosis on this preform.

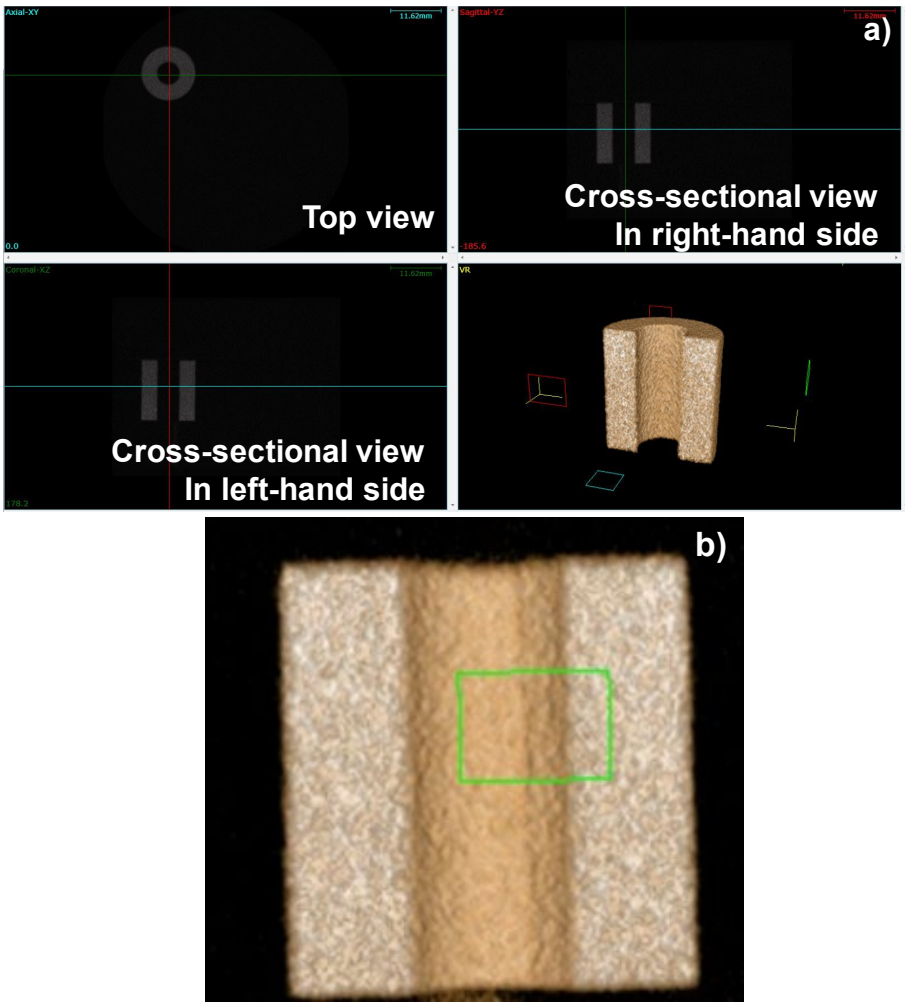

Figure 5. Non-destructive quantitative evaluation on the carbon alignment by X-ray tomography. a) Three dimensional images of preform, and b) half-sectional image of preform.

Fig. 5a depicts the top and cross-sectional view images of green preform. No pores and cavities were detected in every cross-section of preform due to its high relative density. As shown in Fig. 5b, the polyimide powders were consolidated in everywhere.

Sinter-forged polyimide – carbon fiber gear. The preform in the above was fixed into the die-cavity with the shape of fifteen-teeth gear. At first, the preform was viscously deformed from a cylindrical shape to a fifteen-teeth gear during hot forging, as illustrated in Fig. 2. The holding die temperature was 623 K (350 °C), the duration was 180 s, and the applied load was 2 kN. After this hot forging, the die temperature is increased from 623 K to 693 K (420 °C) for sinter-forging. At this step, the applied load was varied to 1.5 kN, and the duration was also 180 s. As depicted in Fig. 3, the hot-forged gear model was net-shaped to a gear product.

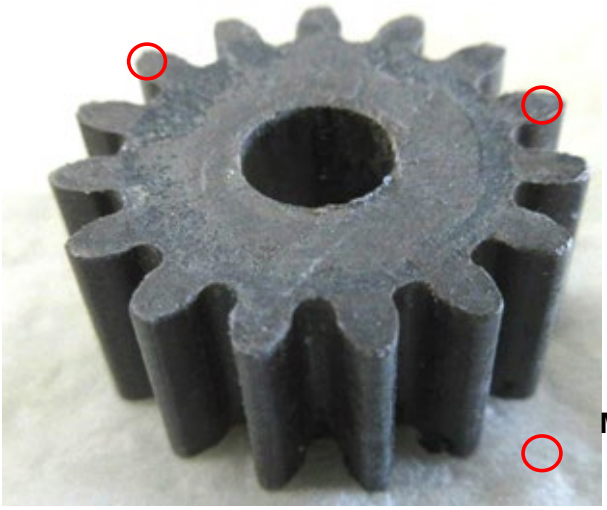

Figure 6. Measurement of Vickers hardness distribution at the tooth top of sinter-forged gear.

Micro-Vickers hardness testing was employed to evaluate the stiffness of sinter-forged gear. As depicted in Fig. 6, the hardness was measured at five positions in each tooth to deduce the average hardness of product. This average hardness reached 180 HV_{1N} much higher than 30 to 50 HV_{1N} for the sinter-forged polyimide gear, reported in [10]. This is because of the carbon fiber reinforcement even at the tops and roots of fifteen gears.

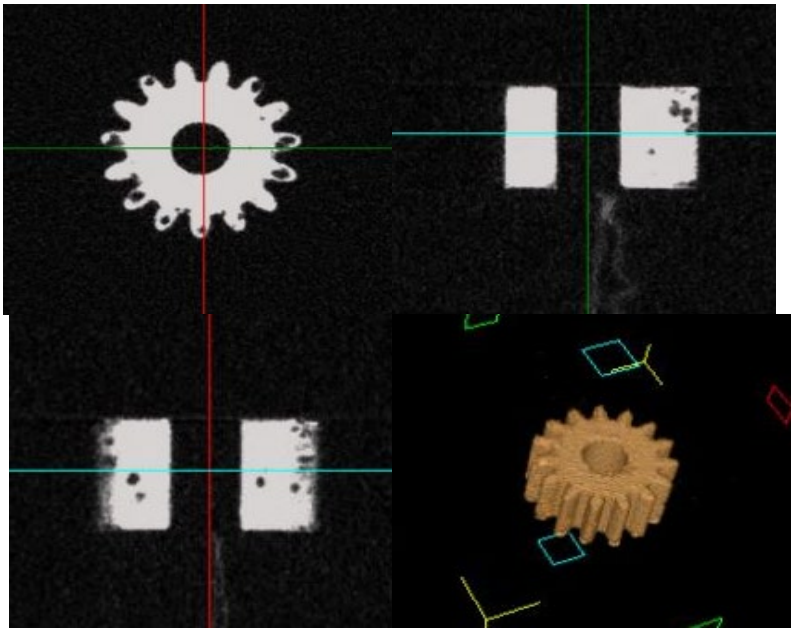

Figure 7. Non-destructive quantitative evaluation on the carbon fiber alignment by X-ray computer tomography.

XCT was also utilized to demonstrate this strengthening of gear teeth by the short carbon fiber reinforcement. Figure 7 also shows the top and cross-sectional view images of sinter-forged gear. Due to the difference of mass density between carbon and polyimide, the carbon fibers were detected as a black dot and a black line. In the top view in Fig. 7, black dots were distinguished in almost all the teeth of gear. This proves that the short-cut carbon fibers were filled into the die cavities together with the polyimide matrix. At the cross-sectional images in Fig. 7, the black dots and lines were also detected so that the whole teeth of gear were reinforced by the short carbon fibers. After SEM analysis, a few carbon fibers, aligning along the gear side surfaces, are detected as a black line and dot in this XCT.

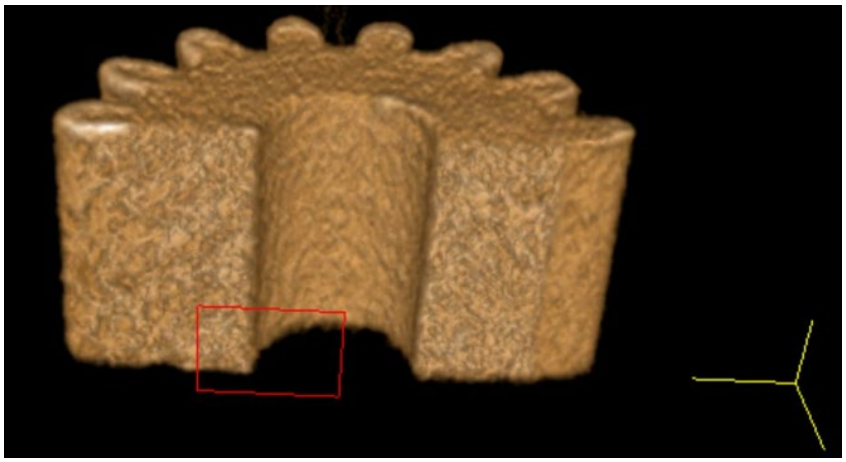

Figure 8. Cross-sectional view image of sinter-forged product by XCT.

Fig. 8 depicts the cross-sectional view image of sinter-forged product. In correspondence to the black dots lines at the top and cross-sectional view image in Fig. 7, the gray-patterns were noticed in Fig. 8. This proves that a short carbon fiber distributes and orients by itself in the polyimide matric of gear teeth.

Carbon fiber mass-fraction effect on the forging process. The green preform, the hot-forged gear model, and the sinter-forged product with the different mass fraction of carbon fibers are compared among them to investigate the carbon fiber mass-fraction effect on the two-step forging process,

Figure 9. Green compact, hot-forged and sinter-forged gears including the carbon fibers by 1 mass% into polyimide powders. The white colored depots were residual solid lubricants of hBN (hexagonal boron nitride) powders.

Fig. 9 depicts the green preform, the hot-forged gear model, the sinter-forged gear product, only including the carbon fibers with 1 mass%. As seen in the green compact, the short carbo fibers are detected as a black dot. This preform was forged at 623 K for 180 s under the applied load of

2 kN. During this hot forging process, the polyimide matrix deforms visco-plastically to fill into the fifteen teeth cavities. Using the hBN as a solid lubricant at the elevated temperature, the hot forging process is free from adhesion of gear-model and gear-product onto the die surfaces.

Let us compare the effect of carbon mass fraction on the three-step process. As shown in Figs. 10 and 11, more black dots are detected on the surface of preform. When adding the carbon fraction by 3 mass%, every surface of hot-forged gear model and sinter-forged gear product is formed to be smooth with the highest accuracy in dimension. When increasing the fraction up to 5 mass%, some of fibers are located near the surface to roughen the finished surface and to increase the surface roughness of models and products. To be discussed in later, the loading sequence must be changed to an incremental loading with holding time.

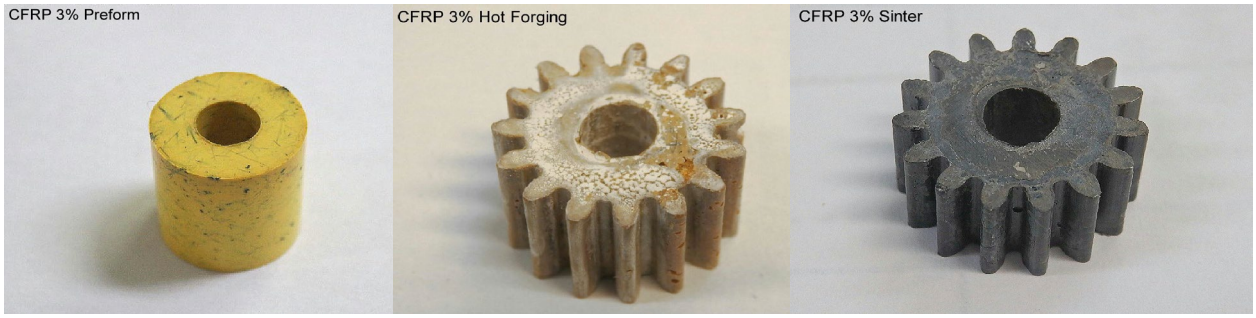

Figure 10. Green compact, hot-forged and sinter-forged gears including the carbon fibers by 3 mass% into polyimide powders.

Figure 11. Green compact, hot-forged and sinter-forged gears including the carbon fibers by 5 mass% into polyimide powders.

Discussion

The mechanical behavior of polyimide matrix as well as the orientation of short-cut carbon fibers are discussed in the powder compaction and the hot-/sinter-forging steps. During the compaction process, each polyimide powder is consolidated to a preform with high relative density of 70 to 80%. Since the initial alignment of short carbon fibers in matrix is fixed by blending and mixing processes before compaction, no essential change occurs in this consolidation. In the hot forging step, the polyimide matrix deforms and flows in the visco-plasticity above the glass-transition temperature. After suggested in [11], the fiber length, its aspect ratio and its geometry influences on the effective visco-plasticity of fiber-matrix composite. Hence, the upsetting and filling processes of polyimide – fiber mixture is driven by more viscous flow than the polyimide without fibers.

XCT images are used to describe the hot forging behavior together with SEM analysis. As shown in Fig. 7, the carbon fibers are seen to agglomerate at the top of teeth as black dots and

lines. This implies that the short carbon fibers are massively pushed into the tooth-cavity of die. That is, the viscous mixtures are filled into the tooth-cavity of die by higher stress gradient from the center of preform to every end of tooth cavity. Relatively longer duration is necessary to this fill-filling of viscous mixture to die cavity.

In the sinter-forging step, the microstructure of hot-forged mixture is homogenized to fix the alignment of carbon fibers in the matrix and to increase the relative density. As depicted in Fig. 8, no porosities are seen in the cross-sectional XCT image; the microstructure becomes uniform without segregation of fibers.

The present XCT has a spatial resolution of 50 μm; local orientation of short carbon fibers is difficult to analyze the original images. In order to describe the local densification and stiffness, finer spatial resolution is necessary. At present, the XCT in the synchrotron-radiation imaging with the use of high intensity X-ray is planned to utilize for this measurement [12]. Under this fine XCT, the local alignment of each short carbon fiber can be analyzed to deduce each orientation of short carbon fiber in the polyimide matrix.

The homogenized finite element analysis [13] is useful to estimate the local stiffness tensor in correspondence to the unit-cell image of XCT-scanned three dimensional image. After [14-15], the unit cell model was determined from the real SEM image of composite materials such as iron ores to calculate its equivalent stiffness and stress distribution in it. This estimate on the homogenized local stiffness tensor is responsible for theoretical validation on the effect of the carbon mass fraction on the hardness.

The orientation of carbon fibers has essential influence on the stiffness and strength of carbon fiber reinforced plastic components. With respect to the reinforcement by the long fibers, the misorientation in the neighboring fibers mainly determines the stiffness of CFRP parts [16]. On the other hand, the statistical distribution of short carbon fibers has main contribution to the stiffness. The unit-cell model is useful in evaluation on the stiffness of CFRSEP gears to represent their elastic stiffness tensor with direct consideration of the microstructure measured by XCT imaging.

The in situ alignment of short-cut carbon fibers in the polyimide matrix during the hot-forging step is identified as a self-orientation process of fibers under the elastic constraint by matrix in the visco-plastic flow. The programmable schedule of external loading in the forging step must be controlled to assist this self-orientation process of fibers to align the fibers along the gear shape. As shown in Figs. 7 and 8, the image-tracing of black dots and lines by XCT enables to describe this self-orientation process with time in loading.

Let us reconsider the marketing of carbon fiber reinforced super-engineering plastic (CFRSEP) gears. The flexible and precise movement of joints in robotics needs the light-weight and small-sized gears with high engineering durability [15, 17]. Due to the carbon fiber reinforcement at the tooth top and root, the tooth-to-tooth traction transfer is put into practice by using the CFRSEP-gears. After early measurement on the gear-grade balancing, the JIS-3 to JIS-5 grades can be attained even in these CFRSEP-gear just like the super-engineering plastic gears in [18]. This dimensional accuracy is sustained even for miniature and mm-sized CFRSEP-gears. These gears must be suitable to micro-systems such as a mobile phone and a sensing micro-robots [19]. Mesoscopic and micro CFRSEP gears grow up to key elements of various micro-systems and devices used for transmitting power and/or motion due to their ultra-light weight, smaller size and compact, higher dimensional accuracy, better functional and operating characteristics, longer service life, zero backlash and ability to sustain their performance under risky ecological environments.

Summary

A manufacturing methodology is proposed to fabricate the miniature carbon fiber reinforced super-engineering plastic gears in mm- to cm-range from the feedstock of polyimide matrix and short-

cut recycled carbon fibers. At first, this feed stock is poured into a die cavity and consolidated to a green preform. In second, this cylindrical preform was fixed into a gear-shaped die cavity of die and hot forged at 623 K for 180 s to a gear model. In third, this mode is further sinter-forged to homogenize its microstructure and yield the gear product with nearly full density. XCT and SEM are utilized to characterize the microstructure of preform, model and product by nondestructive and destructive material evaluation. In particular, the orientation of short carbon fibers to the tooth root and top is detected in the XCT of gear-product. The surface hardness of 180 HV_{1N} than the hardness of 30 HV_{1N} in sintered polyimide gear, proves that carbon reinforcement at the tooth root and top is responsible for this strengthening,

XCT imaging works well to describe the in situ carbon self-orientation during the hot- and sinter-forging processes. Since the spatial resolution in the present XCT is limited by 50 μm, fine imaging on the local alignment of fibers is difficult to analyze in the present study. Only black dots and lines at every tooth in gear model and product, implies that short carbon fibers are placed at every tooth root and top. When increasing this spatial resolution by using the synchrotron-radiation imaging, fine local XCT image is yielded to deduce the unit cell model to represent the equivalent microstructure of CFRSEP-gear. Using the homogenized finite element analysis, the elastic stiffness tensor is calculated from this unit cell model to compare the major elastic moduli in this tensor with the measured hardness of sinter-forged gear product and to provide a way to control the orientation of carbon fibers toward the high stiff and hard gears.

Acknowledgment
The authors would like to express their gratitude to S-I. Kurozumi (Nano-Film Coat, llc.) for his help in experiments.

References

[1] Ando, K., Future prospects and current situation of the robot reduction gear. J. Robotics 33 (5) (2015) pp. 329-333. https://doi.org/10.7210/jrsj.33.329

[2] Souza T. S. G., de Souza M. M., Savoy J., Light-weight assembled gears: A green design solution for passenger and commercial vehicles. Gear Tech. 5 (2013) pp. 64-71.

[3] Z. Liu, Z. You, Z. Wang, Lightweight design of multistage gear reducer based on continuous variables and discrete neighborhood. Proc. ICMD 2017 (2017) 379-387. https://doi.org/10.1007/978-981-10-6553-8_26

[4] Politis D. J., Politis N. J., Lin J., Review of recent developments in manufacturing lightweight multi-metal gears. Production Eng. 15 (2021) pp. 235–262. https://doi.org/10.1007/s11740-020-01011-5

[5] Tatsuno D., Yoneyama T., Kuga M., Honda Y., Akaishi Y., Hashimoto H., Fiber deformation behavior of discontinuous CFRTP in gear forging. Int. J. Material Forming14 (2021) pp. 947-960. https://doi.org/10.1007/s12289-021-01611-1

[6] Tatsuno D., Masukawa H., Forming of CFTRP screw. Proc. JSTP (November 17th, 2023) pp. 315-316.

[7] More C. V., Alsayed Z., Badawi M. S., Thabet A., Pawar P. P., Polymetric composite materials for radiation shielding: a review. Environmental Chemistry Letters 2021, 19, 2057-2090. https://doi.org/10.1007/s10311-021-01189-9

[8] Park S-A., Jeon H., Kim H., Shin S-H., Choy S., Hwang D. D., Koo J. M., Jegal J., Hwang S. Y., Park J., Oh D. X., Sustainable and recyclable super engineering thermoplastic from

biorenewable monomer. Nature Communications. 2919, 10, 2601. https://doi.org/10.1038/s41467-019-10582-6

[9] Aizawa, T, Miyata T., K. Endo, Two-step PM forging for precise fabrication of carbon fiber reinforced engineering plastic gears. Mater. Res. Proc. 28 (2023) pp. 1799-1808. https://doi.org/10.21741/9781644902479-195

[10] Aizawa, T., Miyata, T., Endo, K., Fine sinter-forging of miniature super-engineering plastic gears for carbon fiber reinforcement design. Proc. 5th WCMNM (Chicago, USA; September 19th, 2023) pp. 1-5.

[11] Joung C. G., Phan-Thien N., Fan X. J., Viscosity of curved fibers in suspension. J. Non-Newtonian Fluid Mechanics 102 (1) (2002) pp. 1-17. https://doi.org/10.1016/S0377-0257(01)00163-X

[12] Strotton M. C., Bodey A. J., Wanelik K., Darrow M. C., Medina E., Hobbs C., Rau C., Bradbury E. J., Optimising complementary soft tissue synchrotron X-ray microtomography for reversibly-stained central nervous system samples. Sci. Rep. 8 (2018) 12017. https://doi.org/10.1038/s41598-018-30520-8

[13] Schenk D., Mathis A., Lippuner K., Zysset P., In vivo repeatability of homogenized finite element analysis based on multiple HR-pQCT sections for assessment of distal radius and tibia strength. Bone 141 (2020) 115575. https://doi.org/10.1016/j.bone.2020.115575

[14] Aizawa T., Suwa Y., Muraishi S., Real microstructure modeling for stiffness and strength analyses of texture in ores. ISIJ-International 44 (12) (2004) pp. 2086-2092. https://doi.org/10.2355/isijinternational.44.2086

[15] Aizawa T., Suwa Y., Meso-porous modeling for theoretical analysis of sinter ores by the phase-field, unit-cell method. ISIJ-International 45 (4) (2005) pp. 587-593. https://doi.org/10.2355/isijinternational.45.587

[16] Lomov S. V., Fiber mis-orientation identified via XCT and structure tensor-based image analysis. ESAFORM2023-Webinar (September 20th, 2023).

[17] Hashimoto K., Mechanics of humanoid robot. Advanced Robotics 34 (21-22) (2020) pp. 1390-1397. https://doi.org/10.1080/01691864.2020.1813624

[18] Aizawa T., Miyata T., Endoh K., Two-step PM-procedure for fabrication of super-engineering plastic gears. J. Machines (2024) (in press). https://doi.org/10.3390/machines12030174

[19] Chaubey S. K., Jain B. K., State-of-art review of past research on manufacturing of meso and micro cylindrical gears. Precision Engineering 51 (2018) pp. 702-728. https://doi.org/10.1016/j.precisioneng.2017.07.014